NASA Contractor Report 178011
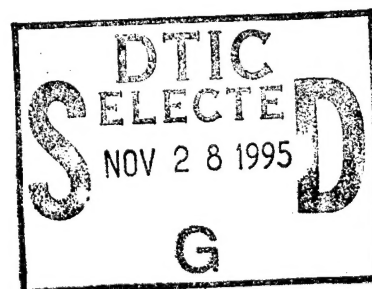
AUTOCLAVE PROCESSING FOR COMPOSITE MATERIAL
FABRICATION - I. AN ANALYSIS OF RESIN FLOWS
AND FIBER COMPACTIONS FOR THIN LAMINATES

T. H. Hou

PRC Kentron, Inc.

Aerospace Technologies Division

Hampton, Virginia 23666

DTIC
SELECTED
NOV 2 8 1995
G

DTIC QUALITY INSPECTED 5

NASA
National Aeronautics and
Space Administration

Langley Research Center
Hampton, Virginia 23665

JAN 1986
RECEIVED
NASA STI FACILITY
ACCESS DEPT.

PLASTEC

DEPARTMENT OF DEFENSE
PLASTICS TECHNICAL EVALUATION CENTER
ARRADCOM, DOVER, N. J.

19951122 008

--   1   OF   1
--   ***DTIC DOES NOT HAVE THIS ITEM***
-- 1 - AD NUMBER: D440351
-- 5 - CORPORATE AUTHOR: KENTRON INTERNATIONAL INC HAMPTON VA*
-- 6 - UNCLASSIFIED TITLE: AUTOCLAVE PROCESSING FOR COMPOSITE MATERIAL
--   FABRICATION - I. AN ANALYSIS OF RESIN FLOWS AND FIBER COMPACTIONS
--   FOR THIN LAMINATES.
-- 9 - DESCRIPTIVE NOTE: FINAL REPT.,
--10 - PERSONAL AUTHORS: HOU,T. H. ;
--11 - REPORT DATE: NOV , 1985
--12 - PAGINATION: 33P
--15 - CONTRACT NUMBER: NAS1-18000
--18 - MONITOR ACRONYM: NASA
--19 - MONITOR SERIES: CR-178011
--20 - REPORT CLASSIFICATION: UNCLASSIFIED
--22 - LIMITATIONS (ALPHA):   APPROVED FOR PUBLIC RELEASE; DISTRIBUTION
--   UNLIMITED. AVAILABILITY: NATIONAL TECHNICAL INFORMATION SERVICE,
--   SPRINGFIELD, VA. 22161. NTIS N86-18270.
--33 - LIMITATION CODES: ➤ /

-- END   Y FOR NEXT ACCESSION   END

Autoclave Processing for Composite Material Fabrication
I. An Analysis of Resin Flows and Fiber Compactions for Thin Laminates

TABLE OF CONTENTS

ABSTRACT

High quality long fiber reinforced composites, such as those used in aerospace and industrial applications are commonly processed in autoclaves. An adequate resin flow model for the entire system (laminate/bleeder/breather), which provides a description of the time-dependent laminate consolidation process, is useful in predicting the loss of resin, heat transfer characteristics, fiber volume fraction and part dimension, etc., under a specified set of processing conditions. This could be accomplished by properly analyzing the flow patterns and pressure profiles inside the laminate during processing.

In this paper a newly formulated resin flow model for composite prepreg lamination process is reported. This model considers viscous resin flows in both directions perpendicular and parallel to the composite plane. In the horizontal direction, a squeezing flow between two nonporous parallel plates is analyzed, while in the vertical direction, a poiseuille type pressure flow through porous media is assumed. Proper force and mass balances have been made and solved for the whole system. The effects of fiber-fiber interactions during lamination are included as well. The unique features of this analysis are (i) the pressure gradient inside the laminate is assumed to be generated from squeezing action between two adjacent approaching fiber layers, and (ii) the behavior of fiber bundles is simulated by a Finitely Extendable Nonlinear Elastic (FENE) spring. Favorable comparisons between model predictions and experimental data available in literature are found.

iii

FOREWORD

This work, performed at NASA - Langley Research Center (LaRC), was supported by the LaRC Polymeric Materials Branch (PMB) under Contract NAS1-18000. This is a progress report on an ongoing research project toward monitoring and controls of composite laminate fabrication processing in autoclave. R. M. Baucom (PMB) was the Technical Monitor. This work also represents an extended version of the work entitled "A Theoretical Study of Resin Flows for Thermosetting Materials During Prepreg Processing" previously reported by NASA CR-172442, July, 1984. Thanks are due to James Shen (ODU) who helped to check numerical solutions of Eqs. (9) and (11) as plotted in Figure 5; to Dr. J. A. Hinkley (PMB) who reviewed the entire manuscript prior to its publication.

AUTOCLAVE PROCESSING FOR COMPOSITE MATERIAL FABRICATION
I. AN ANALYSIS OF RESIN FLOWS AND FIBER COMPACTIONS FOR THIN LAMINATES

I. INTRODUCTION

High quality long fiber reinforced composites, such as those used in aerospace and industrial applications, are commonly processed in autoclaves. During processing, the composite materials are subjected to prescribed elevated temperatures and pressures. Selection of a cure cycle (i.e., temperature profile) will dictate the kinetics of the reactive resin matrix, and consequently the profile of chemoviscosity built-up. Increased molding pressure during processing will result in resin flows both perpendicular and parallel to the fibers. The applied pressure helps to consolidate the composite laminates and to squeeze out excess resin and voids. An adequate resin flow model for the entire system (laminate/bleeder/breather), which provides a description of the time-dependent laminate consolidation process, is useful in predicting the loss of resin, heat transfer characteristics, fiber volume fraction and part dimension, etc., under a specified set of processing conditions. This could be accomplished by properly analyzing the flow patterns and pressure profiles inside the laminate during processing.

Considerable work has been conducted in the past by numerous researchers in searching for a relationship between chemoviscosity and cure kinetics [1,2]. However, the mechanics governing the flow of resin associated with the composite lamination process has received little attention. Springer and Loos [3-6] and Lindt [7] had presented pure viscous flow models. In their analyses, the applied pressure during composite prepreg lamination process is carried by the resin matrix only. The pressure gradients resulted inside the

1

laminate create flows in both directions perpendicular and parallel to the planes of the composite. Although favorable comparisons between model predictions and experimental observations have been reported for some cases, it is generally recognized that an adequate flow model for the composite consolidation process must include the effect of compacted fibers as well. Recent measurements [8] indicated that resin pressure could be as low as 1/3 to 1/10 of the applied pressure, and the missing load must be carried by the fibers. Bartlett [9] developed a theoretical flow model for glass-reinforced resin during lamination of multilayer printed circuit boards in the electronic industry. His analysis appeared to be the first attempt to take into account the effects of layers of glass fabric coming into contact with one another as the resin is squeezed out. The model was later compared with experimental results by Bloechle [10,11] using a parallel-plate plastometer, and was successfully applied to quality control of incoming epoxy B-stage prepregs in a manufacturing environment.

More recently Gutowski [12] reported a resin flow/fiber deformation model for composites. By assuming fibers possess small curvatures, an elastic fiber model depicted by a rapidly stiffening spring was constructed. The model was also shown to fit experimental data favorably.

In this paper a newly formulated resin flow model for composite prepreg lamination process is reported. This model considers viscous resin flows in both directions perpendicular and parallel to the composite plane. The effects of fiber-fiber interactions during lamination are included as well. The unique features of this analysis are (i) the pressure gradient inside the laminate is assumed to be generated from squeezing action between two adjacent

2

approaching fiber layers, and (ii) the behavior of fiber bundles is simulated by a Finitely Extendable Nonlinear Elastic (FENE) spring. Comparisons between model predictions and experimental results will also be made.

List of Symbols

c_z	$\equiv dp/dz$ (psi/inch)
ΔE_η	Viscous flow Activation Energy (Kcal/mole)
ΔE_k	Viscosity cure Activation Energy (Kcal/mole)
F	External load (lbs)
$h(t)$	Separation (inch) between parallel plates
h_0	Initial separation (inch) between parallel plates
$\mathring{h}(t)$	$\equiv dh/dt$ (inch/sec)
K	Permeability (inch^2) of porous material
k	Viscosity rate constant
k_∞	Material constant (min^{-1})
p	Pressure (psi) generated by squeezing action between two approaching plates
p_a	Ambient pressure (psi)
p_f	Pressure (psi) absorbed by glass fabric or fiber bundles
Q_1, Q_2	Defined by Eqs. (12), (13)
R_1	Universal gas constant (kcal/mole °K)
r, θ, z	Cylindrical coordinate system
T	Curing temperature (°K)
t	Curing time (sec)
V_0	Velocity (inch/sec) averaged over a small region of space in porous material
V_r, V_z	Velocity (inch/sec) in r and z direction, respectively
z_0	Characteristic thickness (inch) of porous material where resin flows
$\eta(t)$	Chemoviscosity (poise)
η_0	Initial viscosity (poise) at $t = 0$
η_∞	Material constant (poise)
λ	Density (lb/ft^3) averaged over a region in porous material

4

II. THEORY

Physical Model

A simplified idealized schematic diagram of multi-layer composite laminates is shown in Fig. 1. A stack of five layers of prepreg tapes is confined between two steel plates and layers of porous materials. The porous materials include those commonly called bleeder and breather materials. In reality, the fibers are not perfectly straight and aligned as shown. They are rather curved and have indefinite number of points of contact in between. When the laminate compactions occur due to the external load, the number of points of contact among layers of fiber bundles increases rapidly, and so does the fraction of external load carried by the fiber bundles. Such behavior can be conveniently simulated by a non-Hookean elastic spring.

In order to develop a viscous flow model for the resin, a flow channel is postulated and shown schematically in Figure 2(a), where resin is confined between two parallel porous plates separated by a distance, $2h$. Upon application of a force, F, the resin is squeezed outward horizontally and also vertically through the porous media. It is assumed that these two flow directions can be decoupled conceptually as shown in Fig. 2(b) and 2(c). Fig. 2(b) illustrates a squeezing flow between two non-porous plates separated by a same distance, $2h$. A vertical pressure flow through porous materials is illustrated in Fig. 2(c) (assuming no horizontal flow), and that the flow is driven by a pressure drop $(p-p_a)$ across a characteristic distance z_0 where p is the pressure generated by the squeezing action between two approaching plates, and p_a is the ambient pressure. A mass balance between change of plates separation and the flows in these two directions can be established.

5

The externally applied force F must be balanced by the pressures and the elastic force of fiber bundles as well.

Mathematical Formulation

A. Vertical Flow Through Porous Media

For the flow of a fluid through a porous medium, the equation of motion can be replaced by Darcy's law [13]

$$\underline{V}_0 = -\frac{k}{\eta}(\nabla p - \rho g),\tag{1}$$

where the underlined quantities denote vectors. K is the permeability of the porous medium, n is the viscosity. $\underline{V}_0$ is a superficial velocity averaged over a small region of space, and ρ and p are density and pressure, respectivity, averaged over a region available to flow that is large with respect to the pore size.

For an incompressible liquid and constant K and n, Eq. (1) together with the equation of continuity can be reduced to

$$\nabla^2 p = 0\tag{2}$$

As a first order approximation, we assume that Eq. (2) is applicable to our system (Fig. 2(c)) in a unidirectional flow. Eqs. (1) and (2) can then be combined to give

$$V_0 = \frac{K}{\eta} c_z,\tag{3}$$

6

where $c_z = dp/dz$ is a constant. Eq. (3) has also been adopted by Springer and Loos [3-6] in their analysis.

B. Horizontal Squeezing Flow

We now consider the squeezing flow between two non-porous plates, as shown in Fig. 2(b). A cylindrical coordinate system (r,θ,z) is chosen for convenience. The velocity and pressure fields are assumed $V_r = V_r(r,z)$, $V_z = V_z(z)$ and $p = p(r)$ only. The equation of continuity becomes

$$2 \int_0^h V_r \, dz + r (\dot{h} + V_0) = 0,$$ (4)

where $\dot{h} = dh/dt$ is a measure of the speed of approach of the two parallel plates upon the application of force F, and $V_z = \dot{h}$ at $z = h$.

For the velocity field assumed, Bird et al. [14] have shown that the r-component equation of motion can be integrated to give

$$V_r = \frac{h^2 r}{2} \left(- \frac{1}{nr} \frac{dp}{dr}\right) \left[1 - \left(\frac{z}{h}\right)^2\right]$$ (5)

Substituting Eq. (5) into Eq. (4), we have

$$\frac{dp}{dr} = \frac{3}{2} \frac{nr}{h^3} (\dot{h} + V_0),$$ (6)

which can then be integrated to obtain the pressure distribution as

$$p(r) - p_a = - \frac{3}{4} n \frac{R^2}{h^3} (\dot{h} + V_0) \left[1 - \left(\frac{r}{R} \right)^2 \right] \tag{7}$$

Eq. (7) represents the squeezing generated pressure drop between two parallel plates approaching with a speed $\dot{h}(t)$. The pressure distribution is shown to be parabolic, and is dependent upon distance of separation between plates, $h(t)$, and plates approaching speed $\dot{h}(t)$.

Substituting Eq. (6) into Eq. (5), we have

$$V_r(r,z) = - \frac{3}{4} \frac{r}{h} (\dot{h} + V_0) \left[1 - \left(\frac{z}{h} \right)^2 \right]. \tag{8}$$

which describes the velocity profile of flow in the horizontal direction between parallel plates.

C. Elastic Forces from Fiber Bundles

It is recognized that in practice the prepreg tapes are not perfectly straight and aligned within the composite laminate. The fiber bundles are assumed to be curved initially and to behave as an elastic spring. As the force is applied, the number of points of contact in between increases rapidly, and the elastic spring becomes stiffer. Such behavior can be simulated by a Finitely Extendable Nonlinear Elastic (FENE) spring which has a force law of the following form:

$$F_f = P_f \cdot A = k \cdot \frac{(h_0 - h)}{[1 - (\frac{h_0 - h}{h_0 - mR_f})]^n} \tag{9}$$

in which $h(t)$ is the distance of separation between plates, and $h(0) = h_0$ is the initial distance. m and R_f are number and radius of prepreg ply (fiber bundle) respectively. $(h_0 - mR_f)$ then represents the maximum compressible distance achieveable. A is the sample area, k is the elastic constant and n is a constant. A spring (fiber bundles) with this force law will be linear (Hookean) for small compression, but will get stiffer and stiffer as the spring (fiber bundles) is compressed; furthermore, the spring (fiber bundles) cannot be compressed beyond $(h_0 - mR_f)$, because infinitely large compression force is then required according to Eq. (9).

Now we can equate a balance in forces using Eqs. (2), (7), and (9) as follows:

$$F = \int_0^R [p(r) - p_a + c_z z_0 + p_f] \, 2 \, \pi r dr$$

$$= \pi R^2 (C_z z_0 + p_i) - \frac{3}{8} \pi \frac{R^4}{h^3} [n\dot{h} + K c_z] \tag{10}$$

where F is the applied external force to the plates, z_0 is a characteristic length in vertical direction across porous media, and P_f is the pressure absorbed by the fabric or fiber bundles. Physically it is noted that when

layers of fibers come into contact with one another as the resin is squeezed outward, they begin to carry a portion of the applied load. The average pressure applied to the resin is therefore the difference between the average applied pressure and the pressure P_f carried by the fiber bundles.

Eq. (10) can be rearranged as:

$$\frac{dh}{dt} = - \frac{1}{n(t)}\left[K\ c_z + \frac{F-Q_1}{Q_2}\ h^3\right] \tag{11}$$

with

$$Q_1 = \pi R^2\ (c_z z_0 + p_f) \tag{12}$$

and

$$Q_2 = \frac{3}{8}\ \pi R^4 \tag{13}$$

The time-dependent laminate thickness $h(t)$ under a constant load F can therefore be calculated by solving Eq. (11).

10

III. Results and Discussion

For a given multi-layer composite laminate, we have

$$\frac{V_f(t)}{V_f^{0}} = \frac{h_0}{h(t)} \tag{14}$$

where $V_f(t)$, $h(t)$ are the fiber volume fraction and laminate thickness at time t respectively. Similarly $h_0 = h(0)$ and $V_f^{0} = V_f(0)$ are the initial laminate thickness and fiber volume fraction respectively. Substituting Eq. (14) into Eq. (9), we have

$$P_f = k_f \frac{(V_f(t)-V_f^{0})/V_f(t)}{[1 - \frac{(V_f(t)-V_f^{0})/V_f(t)}{(V_f^{f}-V_f^{0})/V_f^{f}}]^{n}} \tag{15}$$

with $k_f = k\, h_0/A$, and V_f^{f} denotes maximum fiber volume fraction obtainable. Experimental data shown in Figure 3 were taken by Gutowski [12]. They were obtained by compressing 6 inch long graphite fiber bundles impregnated in light mineral oil which has a viscosity of 0.05 Pas. The elastic behavior shown is a nonHookean rapidly stiffening spring. By selecting $V_f^{0} = 0.5$, $V_f^{f} = 0.8$, $k_f = 50$, and $n = 1.475$, predictions of FENE spring model, Eq. (15), for the fiber bundles represented by the solid line, are shown to compare favorably with the experimental data in the Figure. During the selection of

11

values for model parameters, it is noted that V_f^0 and V_f^f are obtained from experimental observations, while k_f and n are two adjustable variables.

Bloechle [10] and Bartlett [9] had investigated load/deformation characteristics of a commercial B-stage 1080 glass fabric with a thickness of 0.0036 inch using a parallel-plate plastometer. Measurements of pressure carried by the glass cloth as a function of thickness h are reproduced in Figure 4. By selecting $h_0 = 0.0036$ in., $(h_0-mR_f)/h_0 = 0.99$, $n = 6$, and $k_f = 370$, the FENE model Eq. (9), represented by the solid line, is shown to compare reasonably well with the data points within the experimental range.

The chemoviscosity profile for B-stage 1080 resin under isothermal curing at temperature T had been measured by Bloechle [10], and can be represented by a dual Arrhenius expression as follows:

$$n(t) = n_0 \exp [kt] \qquad (16)$$

with

$$n_0 = n_\infty \exp [\Delta E_n/R_1 T]$$

$$k = k_\infty \exp [-\Delta E_k/R_1 T]$$

where n denotes curing viscosity; n_0 denotes zero time viscosity; k is viscosity rate constant. Values of parameters are tabulated in Table 1.

12

Table 1. Values of parameters for B-stage 1080 epoxy resin and glass fabric

$$n_\infty = 3.78 \times 10^{-13} \text{ poises}$$

$$k_\infty = 5.5 \times 10^9 \text{ min}^{-1}$$

$$\Delta E_n = 28 \text{ kcal/mole}$$

$$\Delta E_k = 20 \text{ kcal/mole}$$

$$R_1 = 1.982 \times 10^{-3} \text{ kcal/(mole } ^\circ K)$$

$$K = 9.0 \times 10^{-13} \text{ inch}^2$$

$$z_0 = 0.0004 \text{ inch}$$

$$R = 2.93 \text{ inch}$$

The flow data obtained by plastometer were performed on 6 x 4.5 inch B-stage specimens under three isothermal cure temperatures of 140, 160, and 180°C. Each of the flow test specimens was comprised of 18 stacked plies. In order to maintain a P/A ratio of 1.16 psi/(sq. inch) which corresponds to a typical MLB lamination procedure utilizing 500 psi on an 18 x 24 inch panel, the applied force F acting on the test specimen was maintained at 845 lbs. The average B-stage thickness per ply $h(t)$ measured for three isothermal flow tests are reproduced in Figure 5. The solid lines are model predictions using Eq. (11) incorporating the FENE spring, Eq. (9), for fibers bundles as discussed above. Values of parameters used in calculations are also included in Table 1.

For a given force F, the model seems to over-estimate the compaction level of the laminate. $C_z z_0$ denotes the pressure drop for flow in vertical direction across a porous medium with a characteristic length z_0. Values of $C_z z_0$ increase with increasing temperature. As the top and bottom bleeders

13

are filled with the resins during processing as a result of vertical flows, it is conceivable that the flow characteristic would change. Uses of variable values of $c_z z_0$ could therefore give better fits between model and experimental data. It is also noted that the range of measured FENE forces P_f, shown in Figure 4, does not cover the experimental values of $h(t)$, shown in Figure 5, where a reduction of only 10-20% of the original laminate thickness been accomplished. The final laminate thickness can, however, be predicted accurately to within 8% at all three curing temperatures.

Fractions of applied load carried by fiber bundles and the reactive resin chemoviscosity as a function of curing time are plotted in Figure 6 and 7 respectively. It is seen that a lower initial viscosity can be obtained for higher isothermal curing condition. A lower viscosity gives rise to a faster plate approach rate $\dot{h}(t)$ at the early stage of laminate compaction, and consequently a higher rate of increase in fractions of applied load carried by the fiber bundles as shown in Figure 6. For small deformation where $(P_f A/F)$ < 1.5%, the force response of FENE spring appears to be Hookean. As the deformation becomes larger, functions of $P_f A/F$ vs. t plotted in Figure 6 should exhibit rapidly increasing slopes corresponding to a rapidly stiffening spring as discussed before. The fact that opposite characteristics for each curve (i.e. decreasing slopes as a function of time in Figure 6) are obtained indicates that the majority of the applied load is carried by the resin matrix which possesses high chemoviscosities for this particular case under discussion.

14

The increases in fiber volume fractions $V_f(t)/V_f^0$ during processing as shown in Figure 8 are calculated from Eq. (14) for three temperatures. By knowing the initial volume fraction of resin, V_r^0, the residual resin volume fraction $V_r(t)$ can be calculated directly from $h(t)$ by the following equation:

$$\frac{V_r(t)}{V_r^0} = \frac{1}{V_r^0}\left[1 - \frac{h_0}{h(t)}\right] + \frac{h_0}{h(t)} \tag{17}$$

The pressure distributions $p(r) - p_a$ for the resin matrix inside the laminate calculated from Eq. (7) are plotted in Figure 9. The distributions are parabolic as a function of radius r. Lower pressure levels as seen for 180°C are consistent with the results shown in Fig. 6, due to the fact that higher portions of the applied load are carried by the fiber bundles. The change in pressure during the lamination process appears to be small for all processing temperatures because of the same reasons discussed before.

15

IV. CONCLUSIONS

A resin flow model for the long fiber reinforced composite prepreg lamination process has been formulated. The model considers viscous resin flows in both directions perpendicular and parallel to the composite plane. The effects of fiber-fiber interactions are included as well. Proper force and mass balances have been made and solved for the entire system which is composed of laminates, bleeders, and breathers. Loss of resin, fiber volume fraction, pressure distribution inside the laminate, part dimensions and temperature effects, etc., as a function of processing time can all be simulated. By assuming proper velocity fields for the squeezing flows between parallel plates, a parabolic pressure distribution within the resin is obtained. The effects of fiber-fiber interactions during laminate compaction are simulated by a Finitely Extendable Nonlinear Elastic (FENE) force, which behaves as a rapidly stiffening spring, and correctly depicts the experimentally observed behaviors of fiber responses during the lamination process. Comparisons of model predictions and one set of experimental data found in the literature show that the final laminate thickness can be predicted accurately to within 8% under various isothermal curing conditions.

16

References

1. Hou, T. H., "On the Applications of WLF Theory for Thermosetting Resins," SPE ANTEC 85 proceedings, 1253-1255, 1985.

2. Roller, M. B., "Characterization of the Time-Temperature-Viscosity Behavior of Curing B-Staged Epoxy Resin," Polym. Engr. Sci., 15, 406, 1975.

3. Springer, G. S., "A Model of Curing Process of Epoxy Matrix Composite Materials," Progress in Science and Engr. of Composites, T. Hayashi, K. Kawata and S. Umekawa Eds., Japan Soc. Composite Matl., 23, 1982.

4. Loos, A. C. and Springer, G. S., "Calculation of Cure Process Variables During Cure of Graphite-Epoxy Composites," Composite Materials: Quality Assurance and Processing, E. C. Browning Ed., ASTM STP 787, 110, 1983.

5. Springer, G. S., "Resin Flow During the Cure Fiber Reinforced Composites," J. Compo. Matl., 16, 400, 1982.

6. Loos, A. C., and Springer, G. S., "Curing of Epoxy Matrix Composites," J. Compo. Matl., 17, 135, 1983.

7. Lindt, J. T., "Engineering Principles of the Formation of Epoxy Resin Composites," SAMPE Quarterly, 14, October 1982.

8. Browning, C. E., Brand, R. A., McKague, E. L., Kardos, E. L., and Dudukovic, M. P., "Processing Science of Epoxy Resin Composites," Industrial Review, General Dynamics Convair Division, San Diego, CA, October 1983.

9. Bartlett, C. J., "Use of the Parallel Plate Plastometer to Characterize Glass-Reinforced Resins: I. Flow Model," Elastomers and Plastics, 10, 369, 1978.

10. Bloechle, D. P., "Use of Parallel Plate Plastometer to Characterize Glass-Reinforced Resins: II. Experimental Results for B-Stage Epoxy Materials," Elastomers and Plastics, 10, 377, 1978.

11. Bloechle, D. P., "Epoxy Prepreg Characterization Using Scaled Flow Testing Techniques," Circuit World, 9, No. 1, 8, 1982.

12. Gutowski, T. G., "A Resin Flow/Fiber Deformation Model for Composites," 30th National SAMPE Symposium Proceedings, 925-934, 1985.

13. Muskat, M., "Flow of Homogeneous Fluids Through Porous Media," McGraw-Hill, 1937.

14. Bird, R. B., Armostrong, R. C., and Hassager, O., "Dynamics of Polymeric Liquids," John Wiley and Sons, 1977.

Composite Processing Laboratory Research Reports

Polymeric Materials Branch, Langley Research Center
National Aeronautics and Space Administration

CPL 1. "A Theoretical Study of Resin Flows for Thermosetting Materials During Prepreg Processing," NASA CR-172442, July 1984, by T. H. Hou (Kentron).

CPL 2. "Chemoviscosity Modeling for Thermosetting Resins - I," NASA CR-172443, November 1984, by T. H. Hou (Kentron).

CPL 3. "Correlation of Dynamic Dielectric Measurements with Viscosity in Polymeric Resin Systems," 30th National SAMPE Symposium and Exhibition, Anaheim, CA., pp. 638-648, March 1985, by D. Kranbuehl, S. Delos, E. Yi, J. Mayer (W&M), T. H. Hou (Kentron), and W. P. Winfree (LaRC).

CPL 4. "On the Applications of WLF Theory to Thermosetting Resins," SPE ANTEC Proceedings, pp. 1253-1255, Washington, D.C., April 1985, by T. H. Hou (Kentron).

CPL 5. "Chemoviscosity Modeling for Thermosetting Resins - II," NASA CR-177958, August 1985, by T. H. Hou (PRC Kentron).

CPL 6. "Autoclave Processing for Composite Material Fabrication - I. An Analysis of Resin Flows and Fiber Compactions for Thin Laminates," NASA CR-178011, November 1985, by T. H. Hou (PRC Kentron).
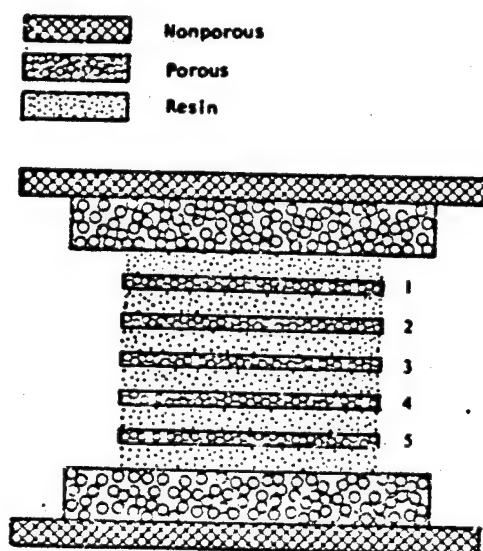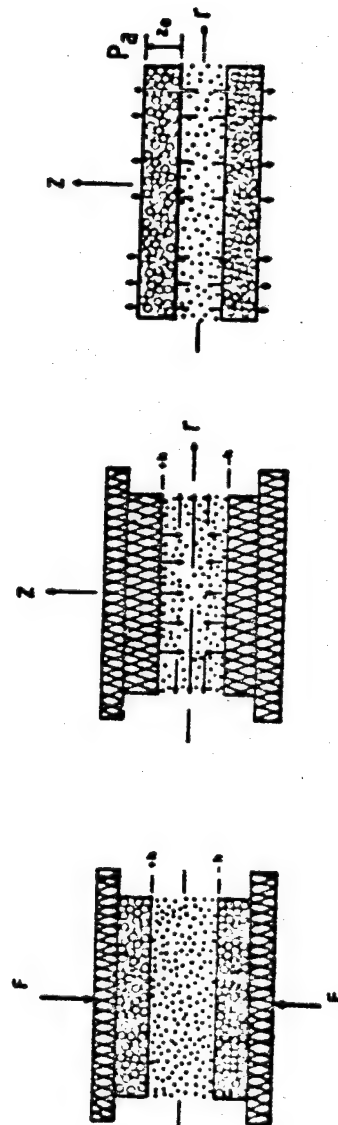
Figure 1. An idealized schematic diagram of multi-layer composite laminates

Figure 2. Physical model for viscous flows in both horizontal and vertical directions during prepreg lamination process

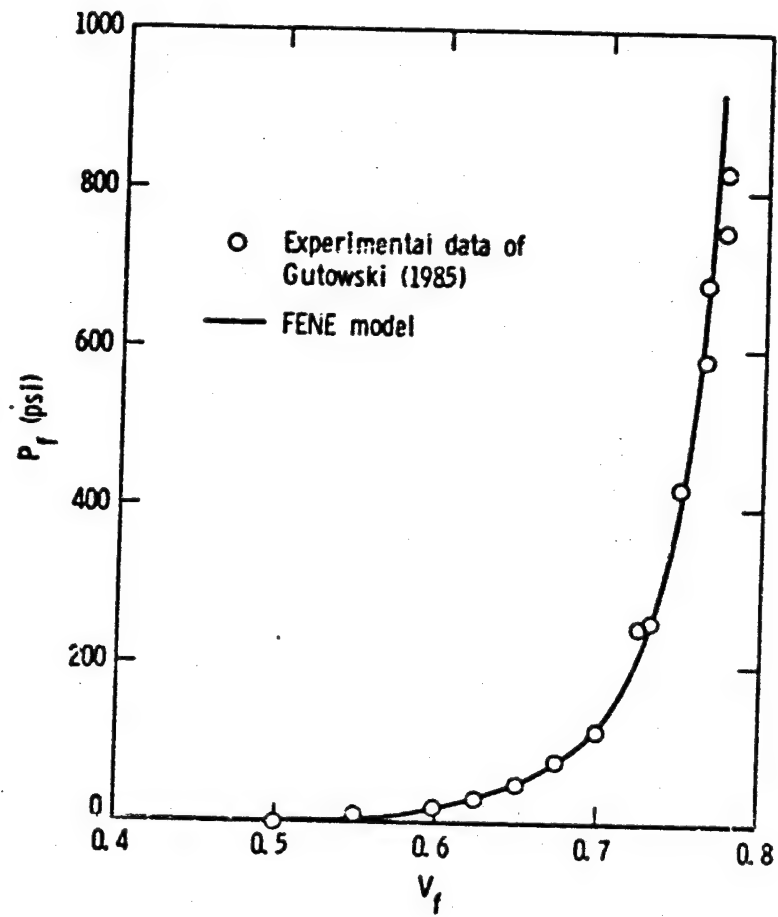(a)   (b)   (c)

nonporous

porous

21

Figure 3. Comparisons between FENE model for the resistance forces of fiber bundles during prepreg lamination process and the experimental data
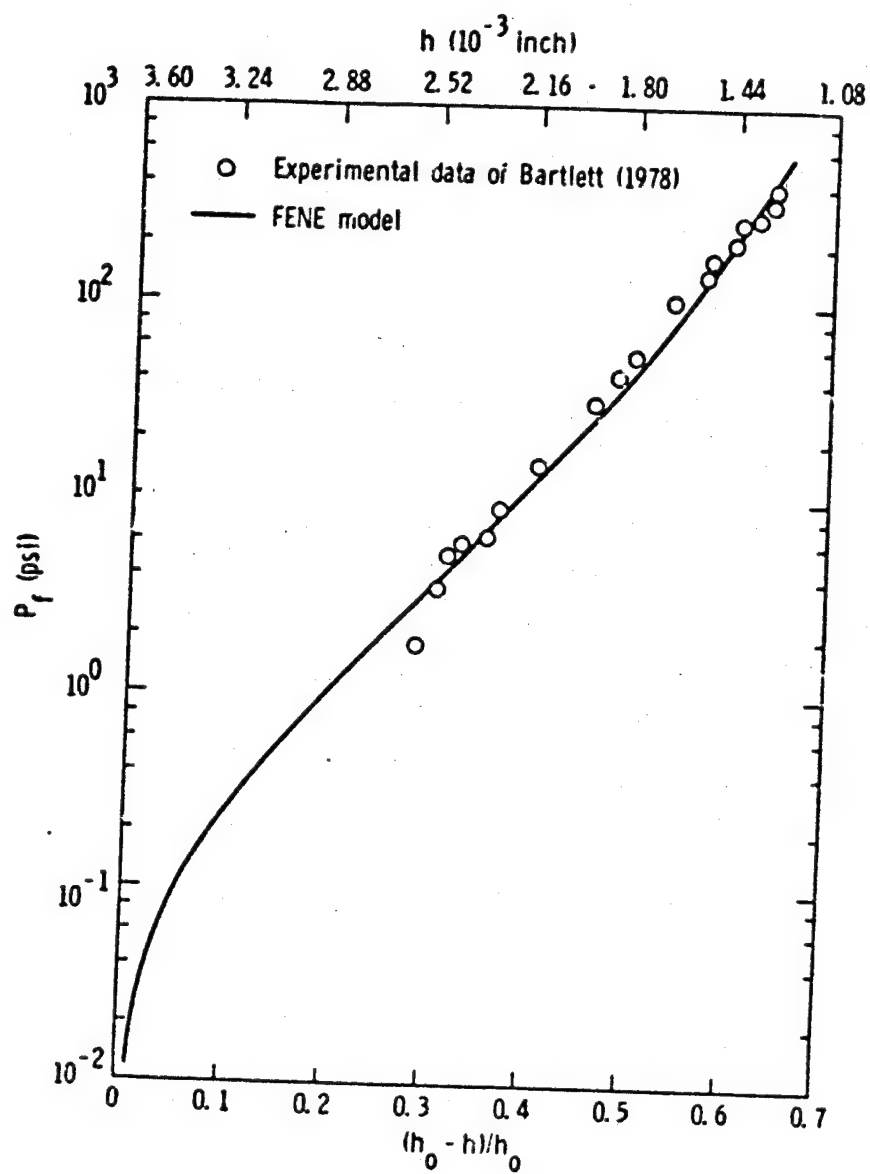
22

Figure 4. Comparisons between FENE model for the resistance forces carried by the glass fabric during lamination process and the experimental data
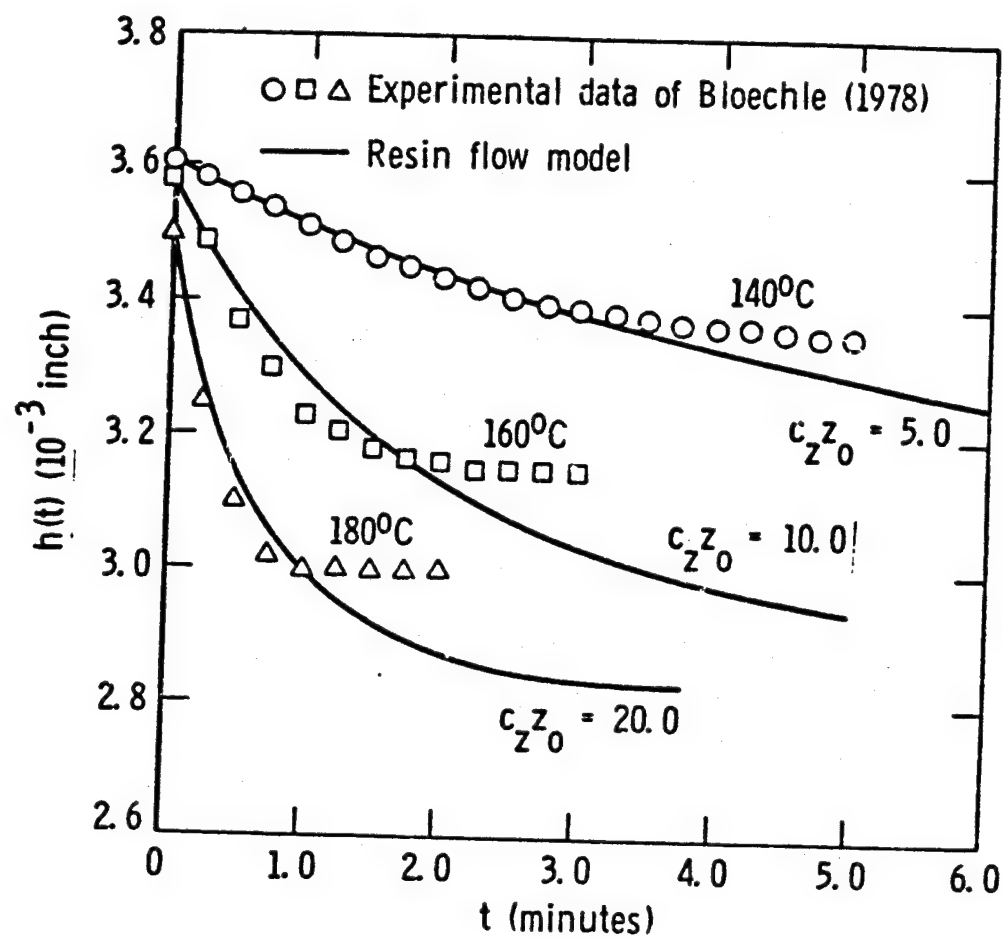
Figure 5. Comparisons between predictions of the resin flow model and the experimental measurements for isothermal processing of B-stage 1080 glass fabric at three different temperatures
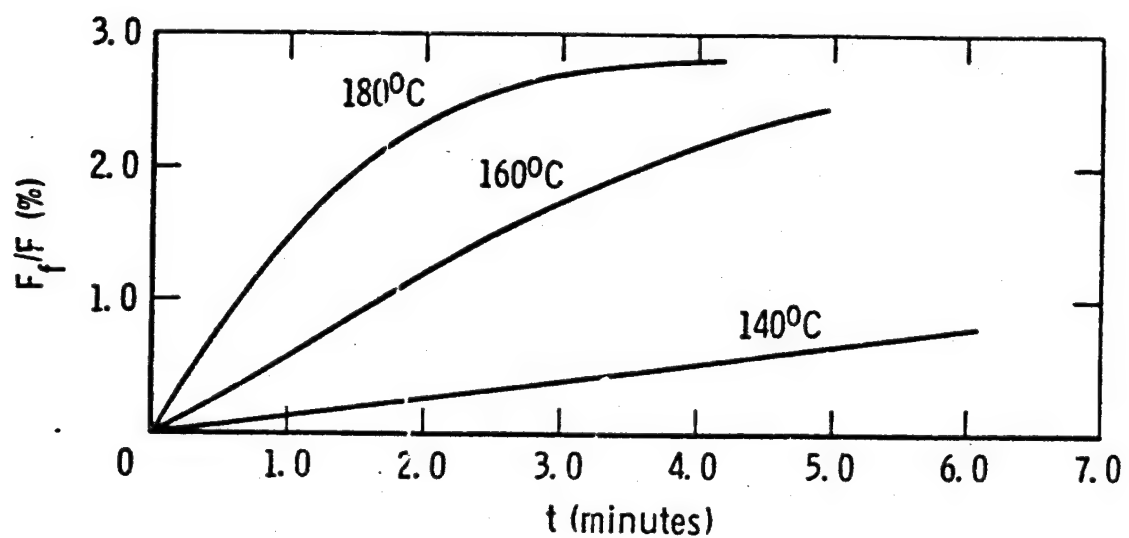
Figure 6. Fractions of applied load carried by the fiber bundles during isothermal processing of B-stage 1080 glass fabric
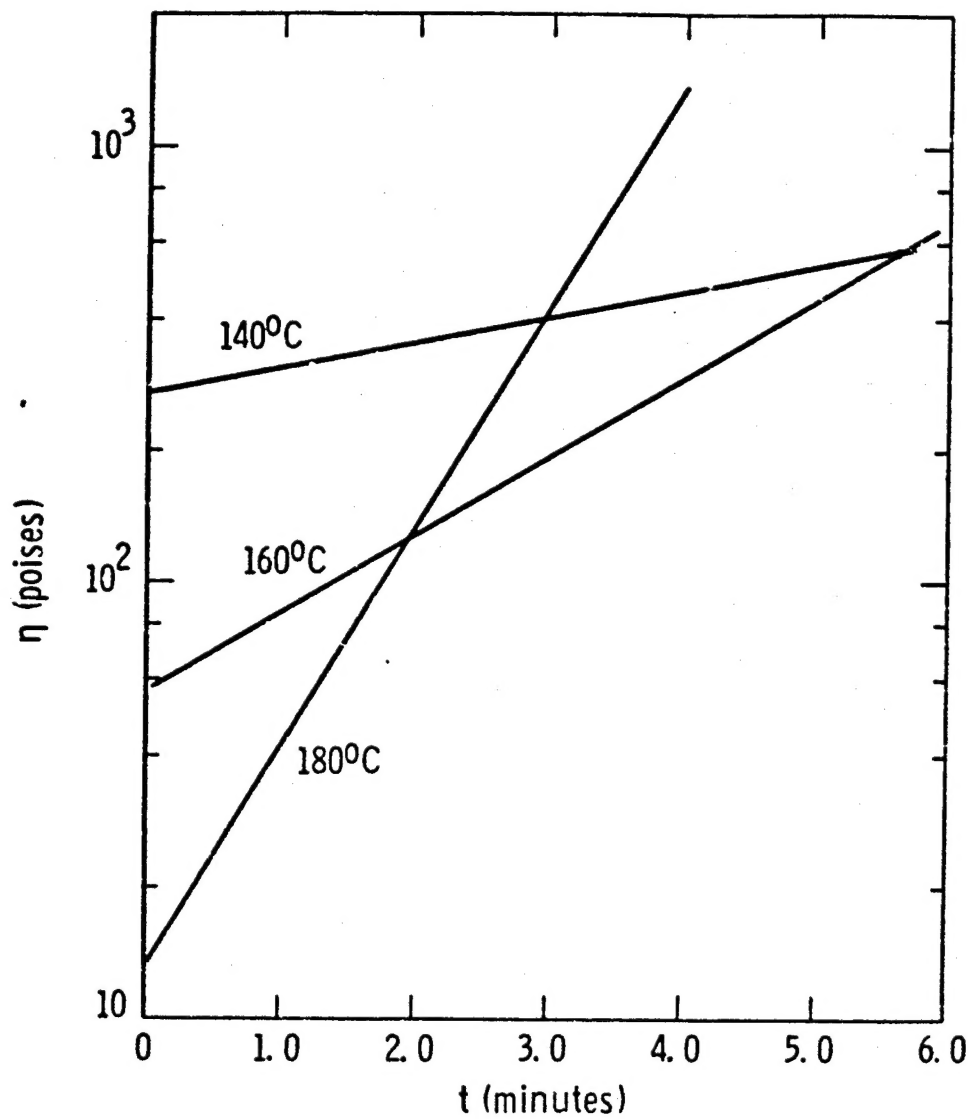
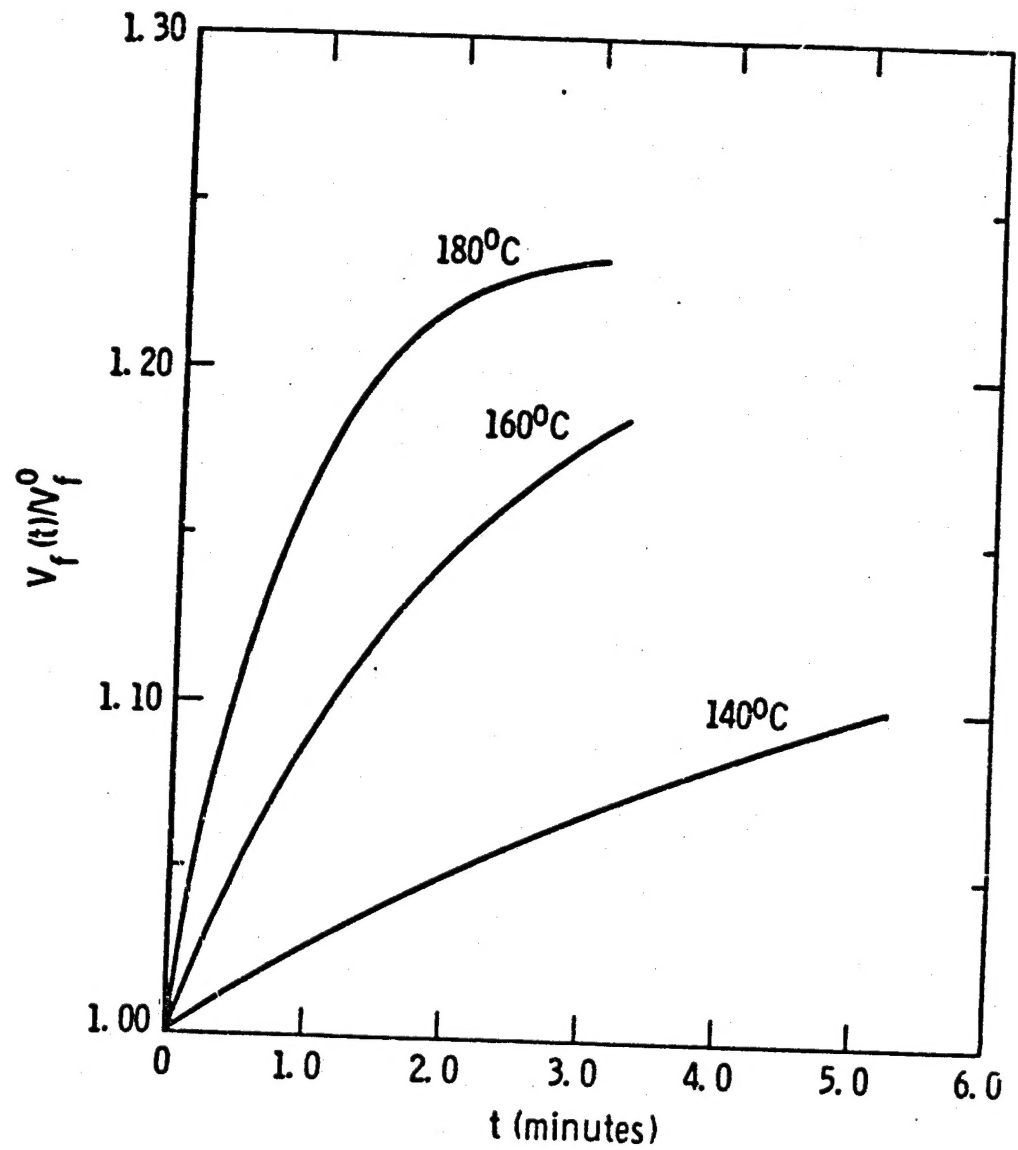Figure 7. Chemoviscosity profiles for isothermal curing of B-stage epoxy resin [9] at three temperatures

Figure 8. Changes of fiber volume fractions during isothermal processing of B-stage 1080 glass fabric
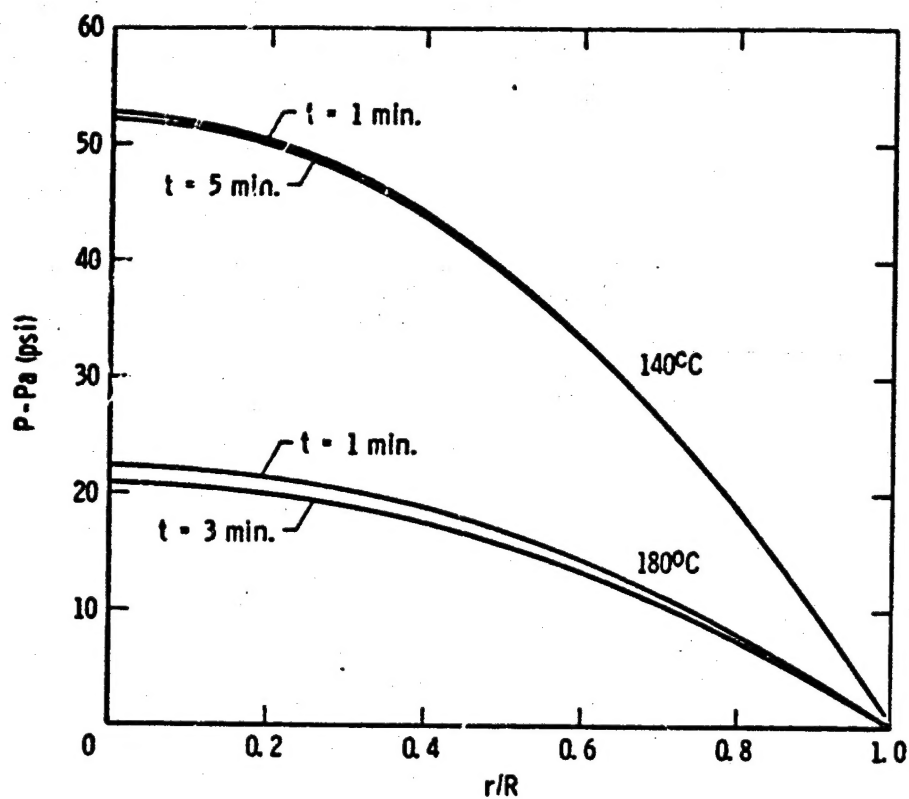
Figure 9. Predicted parabolic pressure distributions which are carried
by the resin matrix inside the multi-layer B-stage 1080 glass
fabric during isothermal curing at two different temperatures

1. Report No. NASA CR- 178011	2. Government Accession No.	3. Recipient's Catalog No.
4. Title and Subtitle Autoclave Processing for Composite Material Fabrication - I. An Analysis of Resin Flows and Fiber Compactions for Thin Laminate		5. Report Date November 1985
		6. Performing Organization Code
7. Author(s) T. H. Hou		8. Performing Organization Report No.
9. Performing Organization Name and Address PRC Kentron, Inc. Aerospace Technologies Division 3221 N. Armistead Avenue Hampton, VA 23666		10. Work Unit No.
		11. Contract or Grant No. NAS1-18000
12. Sponsoring Agency Name and Address National Aeronautics and Space Administration Washington, DC 20546		13. Type of Report and Period Covered Contractor Report
		14. Sponsoring Agency Code 505-63-01-01

15. Supplementary Notes

Langley Technical Monitor: R. M. Baucom
Final Report

16. Abstract

High quality long fiber reinforced composites, such as those used in aerospace and industrial applications are commonly processed in autoclaves. An adequate resin flow model for the entire system (laminate/bleeder/breather), which provides a description of the time-dependent laminate consolidation process, is useful in predicting the loss of resin, heat transfer characteristics, fiber volume fraction and part dimension, etc., under a specified set of processing conditions. This could be accomplished by properly analyzing the flow patterns and pressure profiles inside the laminate during processing.

In this paper a newly formulated resin flow model for composite prepreg lamination process is reported. This model considers viscous resin flows in both directions perpendicular and parallel to the composite plane. In the horizontal direction, a squeezing flow between two nonporous parallel plates is analyzed, while in the vertical direction, a poiseuille type pressure flow through porous media is assumed. Proper force and mass balances have been made and solved for the whole system. The effects of fiber-fiber interactions during lamination are included as well. The unique features of this analysis are (i) the pressure gradient inside the laminate is assumed to be generated from squeezing action between two adjacent approaching fiber layers, and (ii) the behavior of fiber bundles is simulated by a Finitely Extendable Nonlinear Elastic (FENE) spring. Favorable comparisons between model predictions and experimental data available in literature are found.

17. Key Words (Suggested by Author(s)) Thermoset, Squeezing Flow, Laminate Compaction, Plastometer, Resin Flow Model	18. Distribution Statement Unclassified - Unlimited Subject Category 24	
19. Security Classif. (of this report) Unclassified	20. Security Classif. (of this page) Unclassified	21. No. of Pages 34 / 22. Price A03